Integrated analysis of tertiary lymphoid structures in relation to tumor-infiltrating lymphocytes and patient survival in pancreatic ductal adenocarcinoma

Tanaka, Takeshi ; Masuda, Atsuhiro ; Inoue, Jun ; Hamada, Tsuyoshi ; Ikegawa, Takuya ; Toyama, Hirochika ; Sofue, Keitaro ; Shiomi, Hideyuk…

(Citation)
Journal of Gastroenterology,58(3):277-291

(Issue Date)
2023-03

(Resource Type)
journal article

(Version)
Accepted Manuscript

Integrated Analysis of Tertiary Lymphoid Structures in Relation to Tumor-infiltrating Lymphocytes and Patient Survival in Pancreatic Ductal Adenocarcinoma

Takeshi Tanaka[1], Atsuhiro Masuda[1*], Jun Inoue[1], Tsuyoshi Hamada[2], Takuya Ikegawa[1], Hirochika Toyama[3], Keitaro Sofue[4], Hideyuki Shiomi[1], Arata Sakai[1], Takashi Kobayashi[1], Shunta Tanaka[1], Ryota Nakano[1], Yasutaka Yamada[1], Shigeto Ashina[1], Masahiro Tsujimae[1], Kohei Yamakawa[1], Shohei Abe[1], Masanori Gonda[1], Shigeto Masuda[1], Noriko Inomata[1], Hisahiro Uemura[1], Shinya Kohashi[1], Kae Nagao[1], Maki Kanzawa[5], Tomoo Itoh[5], Yoshihide Ueda[1], Takumi Fukumoto[3] and Yuzo Kodama[1]

[1] Division of Gastroenterology, Department of Internal Medicine, Kobe University Graduate School of Medicine, 650-0017, Japan

[2] Department of Gastroenterology, Graduate School of Medicine, The University of Tokyo, Tokyo, 113-8655, Japan

[3] Division of Hepato-Biliary-Pancreatic Surgery, Department of Surgery, Kobe University Graduate School of Medicine, 650-0017, Japan

[4] Department of Radiology, Kobe University Graduate School of Medicine, 650-0017, Japan

[5] Division of Diagnostic Pathology, Kobe University Graduate School of Medicine, 650-0017, Japan

Short Title: TLS in Pancreatic Cancer

Word count: 6993 (including references)

***Correspondence:**

Atsuhiro Masuda, M. D, Ph.D

Division of Gastroenterology, Department of Internal Medicine,

Kobe University Graduate School of Medicine

7-5-1 Kusunoki-cho, Chuo-ku, Kobe, Hyogo, 650-0017, Japan

Telephone: +81-78-382-6305; Fax: +81-78-382-6309

E-mail: atmasuda@med.kobe-u.ac.jp

Disclosures: The authors declare no potential conflicts of interest.

Financial Support: This work was supported by JSPS KAKENHI (Grants-in-Aid for Scientific Research), Grant No.19K08444 (A.M.), and Grant No.19H03698 (Y.K.). This work was also supported by Pancreas Research Foundation of Japan (A.M.).

Author contributions:

All authors contributed to the study conception and design. Material preparation, data collection and analysis were performed by Takeshi Tanaka, Jun Inoue, Takuya Ikegawa, Shunta Tanaka, Ryota Nakano, Yasutaka Yamada, Shigeto Ashina, Masahiro Tsujimae, Kohei Yamakawa, Shohei Abe, Masanori Gonda, Shigeto Masuda, Noriko Inomata, Hisahiro Uemura, Shinya Kohashi and Kae Nagao. The first draft of the manuscript was written by Takeshi Tanaka, and Atushiro Masuda designed the study concept, analyzed data, and wrote the manuscript. Maki Kanzawa and Tomoo Itoh reviewed all slides in the study and advised on pathological diagnosis as needed. Tsuyoshi Hamada, Hirochika Toyama, Keitaro Sofue, Hideyuki Shiomi, Arata Sakai, Takashi Kobayashi, Yoshihide Ueda, Takumi Fukumoto and Yuzo Kodama were involved in study supervision and revised the manuscript. All authors read and approved the final manuscript.

Abstract

Background

Tertiary lymphoid structure (TLS) reflects an intense immune response against cancer, which correlates with favorable patient survival. However, the association of TLS with tumor-infiltrating lymphocytes (TILs) and clinical outcomes has not been investigated comprehensively in pancreatic ductal adenocarcinoma (PDAC).

Methods

We utilized an integrative molecular pathological epidemiology database on 162 cases with resected PDAC, and examined TLS in relation to levels of TILs, patient survival, and treatment response. In whole-section slides, we assessed the formation of TLS and conducted immunohistochemistry for tumor-infiltrating T cells (CD4, CD8, CD45RO, FOXP3). As confounding factors, we assessed alterations of four main driver genes (*KRAS*, *TP53*, *CDKN2A* [p16], and *SMAD4*) using next-generation sequencing and immunohistochemistry, and tumor CD274 (PD-L1) expression assessed by immunohistochemistry.

Results

TLSs were found in 112 patients with PDAC (69.1%). TLS was associated with high levels of $CD4^+$ TILs (multivariable odds ratio [OR], 3.50; 95% confidence

interval [CI], 1.65–7.80; *P* = 0.0002), $CD8^+$ TILs (multivariable OR, 11.0; 95% CI, 4.57–29.7, *P* < 0.0001) and $CD45RO^+$ TILs (multivariable OR, 2.65; 95% CI, 1.25–5.80, *P* = 0.01), but not with levels of $FOXP3^+$ TILs. TLS was associated with longer pancreatic cancer-specific survival (multivariable hazard ratio, 0.37; 95% CI, 0.25–0.56, *P* < 0.0001) and favorable outcomes of adjuvant S-1-treatment. TLS was not associated with driver gene alterations but tumor CD274 negative expression.

Conclusions

Our comprehensive data supports the surrogacy of TLS for vigorous anti-tumor immune response characterized by high levels of helper and cytotoxic T cells and their prognostic role.

Keywords: tertiary lymphoid structures, tumor-infiltrating lymphocytes, neutrophil-to-lymphocyte ratio, pancreatic ductal adenocarcinoma

Introduction

Pancreatic ductal adenocarcinoma (PDAC) remains one of the most lethal malignancies among all cancer types. The overall 5-year survival rate is approximately 20 % because of the high recurrence rate in patients with PDAC who undergo curative resection [1]. In general, tumor progression and metastasis formation depend on not only genetic and epigenetic alterations of cancer cells but also the tumor microenvironment (TME) including immune cells [2]. TME is involved in shaping the cellular fate of tumor-infiltrating lymphocytes (TILs) and the efficacy of the anti-tumor treatment [3]. Evidence showed that the immune network including TILs and systemic immune responses play a pivotal role in carcinogenesis and prognosis in PDAC [4-6]. Especially, tumor-infiltrating $CD8^+$ T cells are immune effector cells that can eliminate cancer cells [4]. TIL-associated cytotoxic immune responses via tumor neoantigen presentation boost the cancer-immunity cycle, resulting in broad and systemic immune activation. Typically, these local and systemic immune responses against cancer are regulated by secondary lymphoid organs (SLOs), such as regional lymph nodes of cancer [7]. Recent studies suggest that these immune responses might also be modulated by lymphoid aggregates called tertiary lymphoid structure (TLS) [8].

TLS is an ectopic lymphoid-like structure without encapsulation and forms at the sites of infection, chronic inflammation, and cancer. In cancer, TLSs are found in the stroma, invasive margin, or core of a tumor and, as well as SLOs, is composed of B-cell follicles, T-cell zones, dendritic cells, and high endothelial venules (HEV) [7, 9]. In some cancers, such as breast [10, 11], lung [12, 13], and colorectal cancer [14, 15], TLS correlates with a favorable prognosis. Thus, TLS might play a pivotal role in local anti-tumor responses. Moreover, TLS in PDAC is associated with a favorable prognosis and outcomes of neoadjuvant chemotherapy [16, 17].

In PDAC, four main genes (*i.e.*, *KRAS*, *TP53*, *CDKN2A* [p16], and *SMAD4*) were identified to be altered in whole-genome analyses [18]. These genes are critical for PDAC progression and are associated with postoperative disease-free survival and overall survival [19]. Recent studies show that specific gene alterations can participate in tumor immune responses in several types of cancer [20-22]. In addition, it has been reported that the programmed death ligand-1 (CD274, PD-L1) expression in cancer cells mediates immunosuppression [23]. However, in PDAC, the influence of the four main driver gene alterations and CD274 (PD-L1) expression on the development of TLS has not yet been

elucidated.

Here, we hypothesized that the TLS might correlate with TILs and systemic immune responses, thereby contributing to favorable prognosis and outcomes of adjuvant chemotherapy in PDAC. To test this hypothesis, we utilized a database of 162 consecutive patients with resected PDAC and performed integrated analysis of TLS in relation to immune status and clinical course.

Methods

Patients and Data Collection

Medical records data on a total of 219 patients with pancreatic carcinoma who underwent pancreatectomy between April 2008 and March 2017 at Kobe University Hospital, Japan, were retrospectively collected. We included conventional PDAC cases by excluding adenocarcinoma originating in intraductal papillary mucinous neoplasms (n = 8), adenosquamous carcinoma (n = 6), anaplastic carcinoma (n = 3), acinar cell carcinoma (n = 1), and mucinous carcinoma (n = 1). The data of remaining 200 conventional PDAC cases was further filtered by excluding cases pertaining to preoperative radiation (n = 6), preoperative chemoradio (n = 3), and distant metastatic PDAC at the time of

surgical resection (n = 15). In addition, cases without formalin-fixed paraffin-embedded (FFPE) samples (n = 14) were excluded. Finally, 162 consecutive histopathologically diagnosed conventional PDAC cases were analyzed. Clinical information collected included age, body mass index (BMI) at surgery, sex, family history of PDAC, alcohol consumption (≤50 g/day or >50 g/day regularly), history of smoking (presence or absence), diabetes mellitus (presence or absence), neoadjuvant chemotherapy (presence or absence), and adjuvant chemotherapy (presence or absence). We also collected information on pathological stage (TNM classification 8^{th} edition), histological grade, and residual tumor status. Hematologic parameters such as absolute lymphocyte counts (ALC), absolute neutrophil counts (ANC), carcinoembryonic antigen (CEA), and carbohydrate antigen 19-9 (CA19-9) were obtained from routine laboratory data within 1 month before surgery without infection. The neutrophil-to-lymphocyte ratio (NLR) was calculated as the serum neutrophil count divided by the serum lymphocyte count. Serum ALC, ANC, and NLR were divided into high and low categories based on the median split. CEA and CA19-9 levels were divided into within normal limits or not.

Regarding the use of tumor samples, informed consent was obtained

at the time of surgery. The study protocol was approved by the Kobe University School of Medicine Ethics Committee, Japan (No.180235). The study was conducted in accordance with the Declaration of Helsinki and the consolidated Good Clinical Practice guidelines (UMIN-CTR ID: UMIN000032917). All authors analyzed the study data and reviewed and approved the final manuscript.

Evaluation of TLS, Quantitative Analysis of TILs, and Evaluation of CD274 (PD-L1) Expression on Cancer Cells

TLSs can be detected within and around the tumor or around the tumor only, using hematoxylin-eosin (H&E) staining. We defined if there are one or more TLS in the whole section, as TLS present, and divided the patients into two groups based on the presence or absence of TLS. Moreover, according to a previous study [16], TLS that developed within and around the tumor was defined as “intratumoral TLS”, while TLS that only developed around the tumor was defined as “peritumoral TLS”. In 10 cases with TLS, components of TLS were assessed using immunohistochemistry (IHC) for $CD4^+$, $CD8^+$, $CD45RO^+$, $FOXP3^+$, $CD68^+$, and $CD20^+$. To analyze the area ratio of the components of these cell populations, TLS was scanned using Adobe Photoshop (Adobe Systems, San Jose, CA, USA).

TILs ($CD4^+$, $CD8^+$, $CD45\ RO^+$, $FOXP3^+$ T cells) were assessed on each IHC slide with the maximum divided surface within and around the tumor tissue, and in normal pancreatic tissue. T cells positive for each marker were counted using Image J software (Java image processing program inspired by National Institute of Health (NIH), USA) in three fields, which were 5mm apart from each other, with maximum lymphocytic infiltration at 200× magnification (count/mm^2). The mean number in three fields was calculated for each case and categorized as high and low densities based on the median split. Representative IHC images for $CD4^+$, $CD8^+$, $CD45RO^+$, and $FOXP3^+$ TILs are shown in Supplementary Fig. 1a.

CD274 (PD-L1) expression was evaluated in the PDAC cells membrane. According to a previous study [24], we divided the patients into two groups: CD274 (PD-L1)-positive or -negative expression. Representative IHC images of CD274 (PD-L1) are shown in Supplementary Fig. 1b. Evaluation of TLS, TILs, and CD274 (PD-L1) expression was performed blinded to the clinical endpoints.

Immunohistochemistry for Immune Markers, PD-L1, and Gene Expression

The slides with the largest area of viable tumor cells selected from each FFPE block were used for IHC. IHC was performed on 5 μm thick tissue sections of each of the above FFPE samples. Immunohistochemical staining for multiple lymphocyte markers was performed using the following antibodies: CD4 (CD4-368-L-CE, clone 1F6, Leica Biosystems, Wetzlar, Germany), CD8 (790-4460, clone SP57, Roche, Ltd., Basel, Switzerland), CD20 (IR604, clone L26, Dako, Santa Clara, CA, USA), CD45RO (AM113-5M, clone UCHL1, BioGenex Laboratories, San Ramon, CA, USA), CD68 (M0876, clone PG-M1, Dako), and FOXP3 (ab20034, clone 236A/E7, Abcam, Cambridge, UK). Immunohistochemical staining for programmed cell death ligand-1 (PD-L1) was performed using the following antibodies: PD-L1 (ab205921, clone 28-8, Abcam). Immunohistochemical staining for protein expression of genes was performed using the following antibodies: p53 (IR616, clone DO-7, Dako), p16 (750-4713, clone E6H4, Roche, Ltd.), and SMAD4 (sc7966, clone B-8, Santa Cruz Biotechnology, Dallas, TX, USA).

Custom-Designed Targeted Sequence Information

The custom-designed targeted sequence of polymerase chain reaction (PCR) amplicons was determined according to the Illumina Custom Protocol (https://www.customprotocolselector.net/cps/Out/10374_80/10374_____.htm). The panel was designed to examine the four main driver genes, viz. *KRAS*, *TP53*, *CDKN2A*, and *SMAD4*. The primer for this targeted custom panel was designed by Illumina DesignStudio (Illumina Inc., Foster City, CA, USA) and consisted of 293 amplicons with an average size of 156 bp and a cumulative targeted region of 45.7 kb. DNA was extracted from FFPE blocks of PDAC using the QIAamp DNA FFPE Tissue Kit (Qiagen, Hilden, Germany) and then extracted DNA was amplified by PCR using a commercial library kit (AmpliSeq for Illumina Library PLUS and Indexes, Illumina Inc.). The pooled libraries were paired-end (2 × 151) sequenced on a micro flow cell with Reagent Kit v2 300 Cycles (Illumina Inc.) on a MiSeq instrument (Illumina Inc.).

Variant Calling and Filtering

The FASTQ files were uploaded to the Illumina genomic cloud computing platform application BaseSpace Sequence Hub (http://www.biomatters.com/apps/melanoma-profiler-for-research), aligned to the

human reference genome hg19. VariantStudio software (version 3.0; Illumina Inc.) was used for variant annotation and filtering. To minimize false positive or false negative variants, including single nucleotide variants (SNVs) and short insertions and deletions (indels) variants, variants with a quality score <30, variant allele frequency (VAF) <1.0%, and coverage <500 were excluded from the analysis [25]. PDAC is characterized by low tumor cellularity [26], and a correlation between tumor cellularity and average VAF of pathogens has been reported [27]. Therefore, a low VAF between 1% and 5% was also included in our analysis. In addition, common variants in the databases of dbSNP, the 1000 Genome Projects and Exome25 Aggregation Consortium, were filtered out according to a previous study [28]. Focusing on variants in the coding region, we excluded all calls in the non-coding region, including the 3'-untranslated region, 5'-untranslated region, intron, downstream, and upstream from further analysis. Additionally, the influence of the variant on the corresponding protein was determined based on SIFT (score < 0.05) and PolyPhen-2 (damaging), and the COSMIC and ClinVar databases were referenced. Based on this filtering, the remaining calls were classified as true mutations. The sequence data reported are available in the DNA Data Bank of Japan (DDBJ) Sequenced Read Archive

under the accession number DRA011317.

Copy Number Variation Detection using Droplet Digital PCR

Copy number variation (CNV) in *TP53*, *CDKN2A*, and *SMAD4* was analyzed using a QX200 Droplet Digital PCR System (Bio-Rad Laboratories, Munich, Germany) according to previously reported method [29]. We carried out droplet digital PCR copy number variation (ddPCR CNV) assays for TP53 (unique assay ID: dHsaCP1000586), CDKN2A (unique assay ID: dHsaCP1000581), SMAD4 (unique assay ID: dHsaCP2500468), and a reference ddPCR CNV AP3B1 assay (unique assay ID: dHsaCP2500348). Similar to a previous study [30], samples that showed <1.4 copy number values, as calculated from the total target and reference event number, were defined as “deletion”.

Final Classification of Gene Alterations of the Four Driver genes

This study analyzed alterations in *KRAS*, *TP53*, *CDKN2A*, and *SMAD4* genes using next-generation sequencing (NGS), ddPCR, and IHC. Using NGS or ddPCR, the cases with SNV, short indels, or CNV were defined as “molecularly altered,” while the cases without SNV, short indels, and CNV were defined as

“molecularly wild.” For *KRAS*, cases were classified as “mutant” or “wild type” based only on NGS. According to previous studies [19, 31], the final classification of gene alterations in *TP53*, *CDKN2A*, and *SMAD4* was analyzed. For *TP53*, all cases showing molecularly altered analyzed using NGS and ddPCR, and cases showing loss of *TP53* protein expression pattern analyzed using IHC were assigned as “altered.” For *CDKN2A* and *SMAD4*, cases showing loss of *CDKN2A* and *SMAD4* protein expression patterns analyzed using IHC were assigned as “altered.” The molecular status of *CDKN2A* and *SMAD4* was confirmed using NGS and ddPCR. *TP53*, *CDKN2A*, and *SMAD4* immunolabeling concurs with 86%, 79%, and 86% concordance with their genetic status, respectively. IHC showed a high concordance rate with the molecular status, as previously reported [32-34]. Representative IHC images for *TP53, CDKN2A*, and *SMAD4* are shown in Supplementary Fig. 1c. All slides from PDAC patients were reviewed by T.I. and subsequently reexamined by a second pathologist (M.K.), with both pathologists unaware of the clinical features of each case. The agreement of IHC assignments for *TP53*, *CDKN2A*, and *SMAD4* was high between the two pathologists, with kappa values of 0.949 ($P < 0.0001$), 0.975 ($P < 0.0001$), and 0.954 ($P < 0.0001$), respectively.

Interferon-Gamma and Interleukin-2 mRNA In Situ Hybridization

The expression level of interferon (IFN)-gamma and interleukin (IL)-2 for TLS-present patients or TLS-absent patients were detected by mRNA in situ hybridization (ISH) using an RNAscope kit (Advanced Cell Diagnostics, Hayward, CA, USA). The IFN-gamma (Cat #310501) and IL-2 (Cat #402041) probes were purchased from Cosmo Bio Company, Limited (Tokyo, Japan). The method recommended by the manufacturer was used for visualizing unstained specimens. To identify that which cells are expressing IFN-gamma mRNA, double IHC/ISH was performed according to previous study [35]. To distinguish between IHC of $CD4^+$ and $CD8^+$ T cells (brown) and ISH of IFN-gamma (pink) more clearly, brown is changed to green using color replacement tools of Photoshop.

Reagents and Cell Lines

Recombinant human IFN-gamma protein (285-IF-100) and recombinant human IL-2 protein (202-IF-010) were purchased from R & D systems (Tokyo, Japan), while 5-fluorouracil (5-FU) was purchased from FUJIFILM (Tokyo, Japan). Human pancreatic adenocarcinoma cell line, AsPC-1, was purchased from

Cosmo Bio Company, Limited (Tokyo, Japan).

Apoptosis Assay

To examine whether cytokine (IFN-gamma and IL-2) or chemotherapy (5-FU) or a combination of these treatments induces apoptosis in a time-dependent manner, the apoptosis level was analyzed using the apoptosis/necrosis detection kit (ab176749, Abcam, Cambridge, UK). The cells were seeded at a density of 15,000 per well in a 96-well plate and cultured for 7 days at 37 °C in a CO_2 incubator. The culture medium was replaced every 48 hours with 200 µl fresh medium with or without IFN-gamma (100 units/mL), IL-2 (500 units/ml), and 5-FU (0.05 mg/mL). The apoptotic cell counts at days 1, 3, 5 and 7 represented the cumulative apoptotic cells detected within the 48-hour period. The cells were stained according to the manufacturer's instructions. The stained cells were photographed using an inverted fluorescent microscope Olympus IX71 at 40× magnification and then were processed with Image J. The error bars indicate one standard deviation (SD). The experiments were performed in triplicate. The data were expressed as mean ± SD.

Statistical Analysis

All statistical analyses were conducted using JMP software (version 12, SAS Institute, Cary, NC, USA), and all *P* values were two-sided. Our primary hypothesis testing was to assess the statistical association between the presence of TLS and TILs ($CD4^+$, $CD8^+$, $CD45RO^+$, $FOXP3^+$ T cells) or systemic immune markers (the levels of serum ALC, serum ANC, and serum NLR). We performed multivariable logistic regression analysis to assess the association of the presence of TLS with TILs or systemic immune markers, adjusting for potential confounders. The binary categorical variable (high and low levels) of TILs and systemic markers was used as an outcome variable. Two models were used for the logistic regression analysis because of the number of outcome variables. The first model was adjusted mainly for clinical characteristics including age, sex, BMI, amount of alcohol consumption, family history of PDAC, history of smoking, diabetes mellitus, serum CA19-9, and serum CEA. The second model was adjusted mainly for tumor characteristics including stage, histology, adjuvant, neo adjuvant, residual tumor status, and alterations in *KRAS, TP53, CDKN2A, and SMAD4*. Backward elimination with a threshold of $P = 0.05$, was used to select variables for the final models. In addition, a Cox hazard model was used for

pancreatic cancer-specific mortality and overall mortality according to the presence or absence of TLS. The multivariable Cox hazard model initially included the same set of the covariates for the multivariable logistic model. Cancer-specific survival (CSS) curves were estimated by the Kaplan-Meier method and differences between patient groups were calculated using the log-rank test. Death of patients from reasons other than PDAC was censored for analyses of cancer-specific mortality. To assess associations between categorical data, the chi-square test (or Fisher's exact test, if appropriate) was performed. To compare mean age and BMI, a *t*-test or analysis of variance (ANOVA), assuming equal variances, was performed. For ISH, the differences in the expression levels of IFN-gamma and IL-2 were examined for statistical significance using Welch's two-sample t-test. For apoptosis assay, the differences among treatment groups were examined for statistical significance using Dunnett's test. All hypothesis tests were 2-sided, and a 2-sided $P < 0.05$ indicated statistical significance.

Results

Characteristics of TLS in PDAC

TLSs were found in 112 patients with PDAC (69.1%); of them, peritumoral TLS

and intratumoral TLS were detected in 85 patients (75.9%) and 27 patients (24.1%), respectively (Fig. 1a). The median number of TLS in the maximum cut surface of the tumor tissue was 3 (range, 1-17). In addition, the median of maximum size and mean size of TLS were 0.11 mm^2 (range, 0,08-0.30) and 0.08 mm^2 (range, 0.04-0.30), respectively. The correlations between TLS and clinical background or tumor features are shown in Table 1. Presence of TLS was associated with a history of smoking (P = 0.02), the normal range of CA19-9 (P = 0.02) and CD274 (PD-L1) negative expression (P = 0.002) but was not associated with the four main driver gene alteration status. In specific *KRAS* mutation pattern, $KRAS^{G12D}$ mutation contributes to the absence of TLS (Supplementary Table 1), but statistical power was limited. The integrated classification of *TP53*, *CDKN2A*, and *SMAD4* are shown in Supplementary Table 2. The components and proportions of several immune cells within the TLS are shown in Figs. 1b and 1c by analyzing 10 cases with TLS. $CD4^+$, $CD8^+$, $CD45RO^+$ T cells were diffusely dominant within TLS, and $CD20^+$ B cells were stained in the center of TLS. In contrast, $FOXP3^+$ T cells and $CD68^+$ macrophages were scattered throughout the TLS. The relationship between TLS and pathological TNM stage, pathological tumor stage, and histological grade is shown in Fig. 1d.

TLS was more abundant in pathological T1 stage than in pathological T2 and T3/T4 stages (P = 0.04), but there were no significant differences between TLS and pathological TNM stage or histological grade. In addition, blood biochemical parameters such as inflammation, nutritional status, and kidney and liver functions were not associated with TLS (Supplementary Table 3).

Correlation Between TLS and TILs or Systemic Immune Markers in PDAC

Within the tumor, the median density of $CD4^+$, $CD8^+$, $CD45RO^+$, and $FOXP3^+$ T cells were 48 (range, 10-301), 140 (range, 13-510), 110 (range, 8-458) and 33 (range, 2 to 213) count/mm^2, respectively; around the tumor, the median levels of $CD4^+$, $CD8^+$, $CD45RO^+$, and $FOXP3^+$ T cells were 21 (range, 9-123), 80 (range, 21-143), 73 (range, 33-169) and 7 (range, 3-115) count/mm^2, respectively. Within the normal pancreatic tissues of the pancreas, the median levels of $CD4^+$, $CD8^+$, $CD45RO^+$, and $FOXP3^+$ T cells were 13 (range, 3-40), 20 (range, 13-43), 11 (range, 2-31) and 4 (range, 2-10) count/mm^2, respectively. Univariate and multivariable logistic regression analyses of the association between TLS and $CD4^+$, $CD8^+$, $CD45RO^+$, and $FOXP3^+$ TILs within the tumor are shown in Table 2. TLS was significantly associated with high levels of $CD8^+$ TILs (multivariable OR

= 9.15, 95% CI = 3.98–23.1, $P < 0.0001$, adjusted for clinical characteristics; OR=11.0, 95% CI = 4.57–29.7, $P < 0.0001$, adjusted for tumor characteristics), with high levels of $CD4^+$ TILs (OR = 4.21, 95% CI = 1.93– 9.74, $P = 0.0002$, adjusted for clinical characteristics; OR = 3.50, 95% CI = 1.65–7.80, $P = 0.001$, adjusted for tumor characteristics) and with high levels of $CD45RO^+$ TILs (OR = 2.51, 95% CI = 1.19– 5.46, $P = 0.02$, adjusted for clinical characteristics; OR = 2.64, 95% CI = 1.24–5.80, $P = 0.01$, adjusted for tumor characteristics). TLS was not associated with $FOXP3^+$ TILs in the multivariable analysis.

The median of ALC and ANC were 1522 and 3251 count/mm^2, respectively. The median of NLR was 2.1. Univariate and multivariable logistic regression analyses of the association between TLS and ALC, ANC, and NLR are shown in Table 3. TLS was significantly associated with high serum ALC (multivariable OR = 2.84, 95% CI = 1.33–6.28, $P = 0.007$, adjusted for clinical characteristics; OR = 2.46, 95% CI = 1.21–5.12, $P = 0.01$, adjusted for tumor characteristics) and with low NLR (OR = 3.21, 95% CI = 1.51–7.10, $P = 0.002$, adjusted for clinical characteristics; OR = 3.15, 95% CI = 1.53–6.72, $P = 0.002$, adjusted for tumor characteristics). TLS was not associated with serum ANC in multivariable analysis.

Prognostic Significance of TLS in PDAC

The median follow-up period was 26 months (range, 1–122 months). Patients with TLS showed a significantly favorable CSS than those without TLS in the Kaplan-Meier analysis (Fig. 2a). Moreover, patients with intratumoral TLS showed a significantly favorable CSS compared with those with peritumoral TLS (P = 0.01) (Supplementary Fig. 2). The median numbers of TLS, the median maximum size, and mean size of TLS were categorized as high and low based on the median split; no association was observed between the number and maximum or mean size of TLS and the patient's prognosis. The multivariable Cox hazard analyses of cancer-specific mortality and overall mortality according to the presence of TLS are shown in Table 4 and Supplementary Table 4, respectively. Among all patients, TLS was an independent prognostic factor for cancer-specific mortality (hazard ratio [HR] = 0.40, 95% CI = 0.26–0.61, P < 0.0001, adjusted for clinical characteristics; HR = 0.37, 95% CI = 0.25–0.56, P < 0.0001, adjusted for tumor characteristics), and overall mortality (HR = 0.45, 95% CI = 0.30–0.68, P = 0.0002, adjusted for clinical characteristics; HR = 0.42, 95% CI = 0.28–0.62, P < 0.0001, adjusted for tumor characteristics). Furthermore, even in late-stage

(stage IIb-III), TLS was an independent prognostic factor for cancer-specific mortality (HR = 0.35, 95% CI = 0.22–0.56, $P < 0.0001$, adjusted for clinical characteristics; HR = 0.33, 95% CI = 0.21–0.52, $P < 0.0001$, adjusted for tumor characteristics) and overall mortality (HR = 0.36, 95% CI = 0.23–0.57, $P < 0.0001$, adjusted for clinical characteristics; HR = 0.35; 95% CI = 0.23–0.54, $P < 0.0001$, adjusted for tumor characteristics).

Prognostic Significance of TILs and Systemic Immune Markers in PDAC

Patients with low NLR and high levels of $CD8^+$ TILs showed a significantly favorable CSS in the Kaplan-Meier analysis (Supplementary Figs. 3a and 3d). The multivariable Cox hazard analyses of cancer-specific mortality and overall mortality according to the TILs and systemic immune markers shown in Supplementary Table 5. High levels of $CD4^+$ TILs, $CD8^+$ TILs, $CD45RO^+$ TILs, high serum ALC, and low NLR were also independent prognostic factors for cancer-specific mortality as well as overall mortality.

Differences of the Cancer-specific Survival in Adjuvant Chemotherapy

TLS-present patients who received adjuvant chemotherapy with tegafur-

gimeracil-oteracil potassium capsules (S-1), which is a 5-FU based agent, had significantly longer CSS compared with those treated with gemcitabine or receiving no chemotherapy (*P* = 0.02, Fig. 2b). This effect was not observed in the TLS-absent cases (Fig. 2c). The background characteristics of the patients in each group are shown in Supplementary Table 6. Among the different treatment groups, there were significant differences in age (*P* = 0.007), BMI (*P* = 0.02), history of smoking (*P* = 0.006), and residual tumor status (*P* = 0.003). Therefore, we performed multivariable Cox hazard analyses adjusted for age, BMI, history of smoking, and residual tumor status. In addition to Kaplan-Meier analysis, patients who received S-1 adjuvant chemotherapy had a significantly favorable prognosis compared with the absence of chemotherapy in TLS-present cases (multivariable HR = 0.51, 95% CI = 0.26–0.97, *P* = 0.04, Table 5), but not in TLS-absent cases. In addition, patients with low NLR who received S-1 adjuvant chemotherapy had significantly longer CSS (*P* = 0.0001, Supplementary Fig. 3b), but not in patients with high NLR (Supplementary Fig. 3c). In cases with high level of $CD8^+$ TILs, there was no significant difference of CSS, but S-1 adjuvant chemotherapy tended to prolong prognosis (Supplementary Fig. 3e). On the other hand, in cases with low level of $CD8^+$ TILs, the absence of chemotherapy

tended to worsen prognosis (Supplementary Fig. 3f).

To investigate the additional effect of S-1 treatment on TLS-present patients, IFN-gamma and IL-2 mRNA ISH tests were performed in each 5 patients with or without TLS. The expression levels of IFN-gamma and IL-2 in TLS-present patients were higher than those in TLS-absent patients ($P < 0.05$) (Supplementary Fig. 4a, b). Double IHC/ISH showed that IFN-gamma mRNA was localized to $CD4^+$ and $CD8^+$ T cells (Supplementary Fig. 4c). Next, TUNEL assay was performed to assess whether IFN-gamma, IL-2, 5-FU, and their combination can induce the apoptosis of PDAC cell lines. The percentage of apoptotic AsPC-1 cells on day 7 of IFN-gamma was significantly higher than control ($P < 0.01$), and furthermore, combination therapy using IFN-gamma and 5FU was significantly higher than that of IFN-gamma, IL-2, and 5-FU treated cells ($P < 0.001$) (Supplementary Fig. 4d).

Discussion

We found that TLS was significantly associated with high levels of $CD4^+$, $CD8^+$ or $CD45RO^+$ TILs and the activation of systemic immune responses, and these associations may result in longer CSS and favorable outcomes of adjuvant S-1-

treatment. These findings were not associated with tumor molecular characteristics, including the four main driver gene alterations of PDAC, but CD274 (PD-L1) expression in cancer cells is negatively correlated with the development of TLS. TLS shows T cells infiltration and systemic immune response comprehensively and is a simple prognostic marker that can be evaluated using H&E staining.

Hiraoka et al. [16] showed the importance of TLS in T cell priming to enhance local adaptive immunity against PDAC, and that TLS within the tumor might have a higher chance of effector immune cells coming into contact with cancer cells. Previous studies reported high levels of $CD8^+$ TILs in tumor tissues associated with improved prognosis [36, 37]. Therefore, not only the amount of TILs but also the phenotypes of TILs are important for clinical outcomes. $CD8^+$ cytotoxic T-cells (CTL) are essential for tumor elimination, and $CD4^+$ helper T-cells facilitate antigen presentation through cytokine secretion and activation of antigen-presenting cells [38]. $CD45RO^+$ T cells, as memory T cells, are generated during cell-mediated immunity responses. These memory T cells survive for long time after the antigen is eliminated, are responsible for inducing more rapid and amplified responses to second and subsequent exposures to antigens [39].

FOXP3$^+$ regulatory T-cells, inhibit CTL function, promote an anti-inflammatory immune response that might enhance tumor growth [40]. As well as previous studies [13, 16, 41], TLS was associated with high levels of CD4$^+$, CD8$^+$ or CD45RO$^+$ TILs. In addition, these subtypes of TILs were also associated with favorable CSS.

In our study, TLS was associated with history of smoking and negative CD274 (PD-L1) expression. In previous studies [42, 43], the smoking history has been associated with higher tumor-infiltrating immune cells in breast and lung cancer patients. In PDAC, Pineda et al. [44] showed that smoking might increase the incidence of somatic mutations, generate neoantigens, and cause an amplified immunogenicity. Antitumor immune responses induced by smoking might promote TLS development in PDAC. CD274 (PD-L1), an immune checkpoint molecule, is a membrane-bound ligand found on the cell surface of cancer cells and binds to the programmed cell death 1 (PD-1) receptor on T cells, leading to T cell apoptosis and inhibition of T cell activation [45, 46]. The PD-L1/PD-1 axis inhibits anti-tumor immune responses and restrains the cancer-immunity cycle [47]. Thus, the PD-L1/PD-1 axis could be inactivating T cell-related immune responses and the cancer-immune cycle resulting in TLS

development.

The immune system sculpts tumor immunogenicity and provides an environment that contributes to the initiation, progression, and eventual metastasis of cancer [48]. TLS is generally associated with the inhibition of cancer growth and improved prognosis by activating local immune responses [49]. However, tumor-immune interactions are not restricted to the local immune responses but are also influenced with systemic immune responses [48, 50]. TLS is a site for the generation of circulating effector memory cells that control tumor relapse and has been shown to induce systemic long-lasting anti-tumor responses [49]. Farren et al. [50] reported that high levels of antigen-experienced T cells in peripheral blood are a potential positive prognostic factor and suggest the presence of ongoing anti-tumor immune reactions. In breast cancer and colorectal cancer [51, 52], TILs have been reported to influence systemic immune responses. Therefore, as observed here, the local immune responses and systemic immune responses are closely related; presence of TLS is associated with not only $CD4^+$, $CD8^+$, $CD45RO^+$ TILs but also ALC and NLR in PDAC and other cancer types.

The role of TLSs in the adaptive antitumor immune response has been

evaluated; activation of the chemokine-, cytokine-, lymphocyte-, and stromal cell-mediated signaling pathways leads the development of HEV, recruitment of lymphocytes from HEV, and induction of TLS formation [51]. In our study, TLS was associated with longer CSS, moreover we found a favorable outcome by using adjuvant S-1-treatment in TLS-present patients with PDAC. S-1 presents a convenient oral alternative for locally advanced and metastatic pancreatic cancer. S-1 adjuvant chemotherapy significantly extended the overall survival of Japanese patients with resected PDAC [53]. The immune system plays a crucial role in the anti-tumor effects of conventional anticarcinogenic chemotherapy-based treatments [54]. The cytotoxic effect of 5-FU is triggered by the induction of apoptosis in cancer cells and is reported to be enhanced by the IFN-gamma in colorectal cancer [55]. The IFN-gamma is secreted by the activated effector T cells, such as $CD4^+$ and $CD8^+$ T cells [56]. With its cytostatic, pro-apoptotic, and immune-provoking effects, the IFN-gamma plays a central role in the elimination of cancer cells [57]. In our study, IFN-gamma was localized to $CD4^+$ and $CD8^+$ T cells, and the expression level of IFN-gamma in tumor was relatively high in TLS-present PDAC patients, and the combination therapy using 5-FU and IFN-gamma induced the apoptosis of PDAC cell lines in vitro study. Therefore, the synergistic

effect of them may be associated with favorable prognoses in TLS-present PDAC patients. IL-2 is a strong immune growth factor and plays an important role in sustaining the T-cell response [58]; however, no synergistic effect was observed between IL-2 and 5FU.

Recent whole genome analyses of PDAC have revealed a complex mutational landscape: *KRAS*, *TP53*, *CDKN2A*, and *SMAD4* are the four most common gene alterations [18], a recent study has shown that the generated neoantigen load caused by somatic alterations in the tumor is associated with immune responses [59]. In PDAC, Pu et al. [60] reported that cases with *KRAS* and *TP53* alterations had significantly worse immune status. On the other hand, Wartenberg et al. [61] reported that the immune-escape status, such as a microenvironment rich in FOXP3 Tregs and poor in T and B cells, is associated with high *SMAD4* and *CDKN2A* alteration rates. In this study, although TLS was not associated with the four main driver gene alteration status, $KRAS^{G12D}$ mutation contributed to the absence of TLS. Cheng et al. [62] reported that the $KRAS^{G12D}$ mutation mediated the upregulation of IL-10 and TGF-β, which inhibit the antitumor immunity in PDAC. Therefore, $KRAS^{G12D}$ mutation in PDAC may inhibit the host immune response including the TLS formation. But the

relationship between tumor genetics and immune status remains controversial, further research is needed to clarify these relationships.

The strength of our study is the near absence of missing data points; preoperative information was collected retrospectively, so the rate of missing items was less than 5% for all variables. The four main driver gene alterations in PDAC were evaluated using NGS and ddPCR as well as IHC. Therefore, the gene alteration status could be evaluated more precisely. However, the present study had some limitations. First, this was a retrospective study, and patients were limited to surgical resection cases. Interpretation of the data may be restricted by selection bias, and it may be unclear whether our data may be applicable to non-surgical cases. Second, the selection of the postoperative treatments depended on the doctor’s choice or the patient’s will. Third, the number of cases in this study was limited, and further large-scale studies are needed to confirm our results.

In conclusion, TLS is one of the major players in anti-tumor immune responses, representing active TILs and systemic immune responses in PDAC. Independent of the four main driver gene alterations, TLS correlates with favorable prognosis and favorable outcomes of adjuvant S-1-treatment. Our

results may be helpful in strategizing therapeutic approaches in treating PDAC.

Acknowledgements

The authors would like to thank Takashi Omori (Clinical & Translational Research Center, Kobe University), Nobuyuki Kakiuchi (Department of Pathology and Tumor Biology, Kyoto University) and Yohei Masugi (Department of Pathology, Keio University School of Medicine) for their valuable comments. We would like to thank Editage (www.edita ge.jp) for the English language editing.

References

1. Mizrahi JD, Surana R, Valle JW, et al. Pancreatic cancer. Lancet 2020;395:2008–20.

2. Quail DF, Joyce JA. Microenvironmental regulation of tumor progression and metastasis. Nat Med 2013;19:1423-37.

3. Ziani L, Chouaib S, Thiery J. Alteration of the Antitumor Immune Response by Cancer-Associated Fibroblasts. Front Immunol 2018;9:414.

4. Foucher ED, Ghigo C, Chouaib S, et al. Pancreatic ductal adenocarcinoma: A strong imbalance of Good and bad immunological cops in the tumor microenvironment. Front Immunol 2018;9:1044.

5. Ino Y, Yamazaki-Itoh R, Shimada K, et al. Immune cell infiltration as an indicator of the immune microenvironment of pancreatic cancer. Br J Cancer 2013;108:914–23.

6. Yang JJ, Hu ZG, Shi WX, et al. Prognostic significance of neutrophil to lymphocyte ratio in pancreatic cancer: a meta-analysis. World J Gastroenterol 2015;21:2807–15.

7. Colbeck EJ, Ager A, Gallimore A, et al. Tertiary Lymphoid Structures in Cancer: drivers of antitumor Immunity, immunosuppression, or Bystander Sentinels in

Disease? Front Immunol 2017;8:1830.

8. Dieu-Nosjean MC, Giraldo NA, Kaplon H, et al. Tertiary lymphoid structures, drivers of the anti-tumor responses in human cancers. Immunol Rev 2016;271:260–75.

9. Ager A. High endothelial venules and other blood vessels: critical regulators of lymphoid organ development and function. Front Immunol 2017;8:45.

10. Martinet L, Garrido I, Filleron T, et al. Human solid tumors contain high endothelial venules: association with T− and B- lymphocyte infiltration and favorable prognosis in breast cancer. Cancer Res 2011;71:5678–87.

11. Lee HJ, Kim JY, Park IA, et al. Prognostic significance of tumor-infiltrating lymphocytes and the tertiary lymphoid structures in HER2-positive breast cancer treated with adjuvant trastuzumab. Am J Clin Pathol 2015;144:278–88.

12. Germain C, Gnjatic S, Tamzalit F, et al. Presence of B cells in tertiary lymphoid structures is associated with a protective immunity in patients with lung cancer. Am J Respir Crit Care Med 2014;189:832–44.

13. Goc J, Germain C, Vo-Bourgais TKD, et al. Dendritic cells in tumor-associated tertiary lymphoid structures signal a Th1 cytotoxic immune

contexture and license the positive prognostic value of infiltrating CD8+T cells. Cancer Res 2014;74:705–15.

14. Di Caro GD, Bergomas F, Grizzi F, et al. Occurrence of tertiary lymphoid tissue is associated with T-cell infiltration and predicts better prognosis in early-stage colorectal cancers. Clin Cancer Res 2014;20:2147–58.
15. Posch F, Silina K, Leibl S, et al. Maturation of tertiary lymphoid structures and recurrence of stage II and III colorectal cancer. Oncoimmunology 2018;7:e1378844.
16. Hiraoka N, Ino Y, Yamazaki-Itoh R, et al. Intratumoral tertiary lymphoid organ is a favourable prognosticator in patients with pancreatic cancer. Br J Cancer 2015;112:1782–90.
17. Kuwabara S, Tsuchikawa T, Nakamura T, et al. Prognostic relevance of tertiary lymphoid organs following neoadjuvant chemoradiotherapy in pancreatic ductal adenocarcinoma. Cancer Sci 2019;110:1853–62.
18. Waddell N, Pajic M, Patch AM, et al. Whole genomes redefine the mutational landscape of pancreatic cancer. Nature 2015;518:495–501.
19. Qian ZR, Rubinson DA, Nowak JA, et al. Association of alterations in main driver genes with outcomes of patients with resected pancreatic ductal

adenocarcinoma. JAMA Oncol 2018;4:e173420.

20. Chen H, Chong W, Teng C, et al. The immune response-related mutational signatures and driver genes in non-small-cell lung cancer. Cancer Sci 2019;110:2348–56.

21. Luen S, Virassamy B, Savas P, et al. The genomic landscape of breast cancer and its interaction with host immunity. Breast 2016;29:241–50.

22. Giannakis M, Mu XJ, Shukla SA, et al. Genomic correlates of immune-cell infiltrates in colorectal carcinoma. Cell Rep 2016;15:857–65.

23. Jiang X, Wang J, Deng X, et al. Role of the tumor microenvironment in PD-L1/PD-1-mediated tumor immune escape. Mol Cancer 2019;18:10.

24. Iwatate Y, Hoshino I, Yokota H, et al. Radiogenomics for predicting p53 status, PD-L1 expression, and prognosis with machine learning in pancreatic cancer. Br J Cancer 2020;123:1253–61.

25. Petrackova A, Vasinek M, Sedlarikova L, et al. Standardization of sequencing coverage depth in NGS: recommendation for detection of clonal and subclonal mutations in Cancer Diagnostics. Front Oncol 2019;9:851.

26. Cancer Genome Atlas Research Network. Electronic address:andrew_a guirre@dfci. harvard.edu, Cancer Genome Atlas Research Network.

Integrated genomic characterization of pancreatic ductal adenocarcinoma. Cancer Cell 2017;32:185–203.e13.

27. Yang SR, Lin CY, Stehr H, et al. Comprehensive genomic profiling of malignant effusions in patients with metastatic lung adenocarcinoma. J Mol Diagn 2018;20:184–94.

28. Suzuki H, Aoki K, Chiba K, et al. Mutational landscape and clonal architecture in grade II and III gliomas. Nat Genet 2015;47:458–68.

29. Mazaika E, Homsy J. Digital droplet PCR: CNV analysis and other applications. Curr Protoc Hum Genet 2014;82:7.24.1–13.

30. Lassaletta A, Zapotocky M, Mistry M, et al. Therapeutic and prognostic implications of BRAF V600E in pediatric low-grade gliomas. J Clin Oncol 2017;35:2934–41.

31. Tsujimae M, Masuda A, Ikegawa T, et al. Comprehensive Analysis of Molecular Biologic Characteristics of Pancreatic Ductal Adenocarcinoma Concomitant with Intraductal Papillary Mucinous Neoplasm. Ann Surg Oncol 2022.

32. Yachida S, White CM, Naito Y, et al. Clinical significance of the genetic landscape of pancreatic cancer and implications for identification of potential

long-term survivors. Clin Cancer Res 2012;18:6339–47.

33. Ohtsubo K, Watanabe H, Yamaguchi Y, et al. Abnormalities of tumor suppressor gene p16 in pancreatic carcinoma: immunohistochemical and genetic findings compared with clinicopathological parameters. J Gastroenterol 2003;38:663–71.

34. Tascilar M, Skinner HG, Rosty C, et al. The SMAD4 protein and prognosis of pancreatic ductal adenocarcinoma. Clin Cancer Res 2001;7:4115–21.

35. Ying S, Humbert M, Barkans J, et al. Expression of IL-4 and IL-5 mRNA and protein product by CD4+ and CD8+ T cells, eosinophils, and mast cells in bronchial biopsies obtained from atopic and nonatopic (intrinsic) asthmatics. J Immunol. 1997;158:3539-44.

36. Vonderheide RH. The Immune Revolution: A Case for Priming, Not Checkpoint. Cancer Cell. 2018;33:563-9.

37. Foucher ED, Ghigo C, Chouaib S, et al. Pancreatic Ductal Adenocarcinoma: A Strong Imbalance of Good and Bad Immunological Cops in the Tumor Microenvironment. Front Immunol. 2018;9:1044.

38. Zitvogel L, Galluzzi L, Kepp O, et al. Type I interferons in anticancer immunity. Nat Rev Immunol. 2015;15:405-14.

39. Hotta K, Sho M, Fujimoto K, et al. Prognostic significance of CD45RO+ memory T cells in renal cell carcinoma. Br J Cancer. 2011;105:1191-6.

40. Tan AH, Goh SY, Wong SC, et al. T helper cell-specific regulation of inducible costimulator expression via distinct mechanisms mediated by T-bet and GATA-3. J Biol Chem. 2008;283:128-136.

41. Masugi Y, Abe T, Ueno A, et al. Characterization of spatial distribution of tumor-infiltrating CD8 + T cells refines their prognostic utility for pancreatic cancer survival. Mod Pathol. 2019;32:1495-1507.

42. Takada K, Kashiwagi S, Asano Y, et al. Clinical verification of the relationship between smoking and the immune microenvironment of breast cancer. J Transl Med. 2019;17:13.

43. Liu C, Xu B, Li Q, et al. Smoking history influences the prognostic value of peripheral naïve CD4+ T cells in advanced non-small cell lung cancer. Cancer Cell Int. 2019;19:176.

44. Pineda S, Maturana EL, Yu K, et al. Tumor-Infiltrating B- and T-Cell Repertoire in Pancreatic Cancer Associated With Host and Tumor Features. Front Immunol.2021;12:730746.

45. Chen DS, Mellman I. Elements of cancer immunity and the cancer-immune

set point. Nature 2017;541:321–30.

46. Dong H, Strome SE, Salomao DR, et al. Tumor-associated B7-H1 promotes T-cell apoptosis: a potential mechanism of immune evasion. Nat Med 2002;8:793–800.

47. Chen DS, Mellman I. Oncology meets immunology: the cancer-immunity cycle. Immunity 2013;39:1–10.

48. Mundry CS, Eberle KC, Singh PK, et al. Local and systemic immunosuppression in pancreatic cancer: targeting the stalwarts in tumor's arsenal. Biochim Biophys Acta Rev Cancer 2020;1874:188387.

49. Sautès-Fridman C, Petitprez F, Calderaro J, et al. Tertiary lymphoid structures in the era of cancer immunotherapy. Nat Rev Cancer 2019;19:307–25.

50. Farren MR, Mace TA, Geyer S, et al. Systemic immune activity predicts overall survival in treatment-naïve patients with metastatic pancreatic cancer. Clin Cancer Res 2016;22:2565–74.

51. Lee KH, Kim EY, Yun JS, et al. The prognostic and predictive value of tumor-infiltrating lymphocytes and hematologic parameters in patients with breast cancer. BMC Cancer 2018;18:938.

52. Huang Y, Lou XY, Zhu YX, et al. Local environment in biopsy better predict the

pathological response to neoadjuvant chemoradiotherapy in rectal cancer. Biosci Rep 2019;39.

53. Uesaka K, Boku N, Fukutomi A, et al. Adjuvant chemotherapy of S-1 versus gemcitabine for resected pancreatic cancer: a phase 3, open-label, randomised, non-inferiority trial (JASPAC 01). Lancet 2016;388:248–57.

54. Zitvogel L, Apetoh L, Ghiringhelli F, et al. Immunological aspects of cancer chemotherapy. Nat Rev Immunol 2008;8:59–73.

55. Adachi Y, Taketani S, Oyaizu H, et al. Apoptosis of colorectal adenocarcinoma induced by 5-FU and/or IFN-gamma through caspase 3 and caspase 8. Int J Oncol. 1999;15:1191-6.

56. Dunn GP, Koebel CM, Schreiber RD. Interferons, immunity and cancer Immunoediting. Nat Rev Immunol. 2006;6:836-48.

57. Kursunel MA, Esendagli G. The untold story of IFN-γ in cancer biology. Cytokine Growth Factor Rev. 2016;31:73-81.

58. Choudhry H, Helmi N, Abdulaal WH, Prospects of IL-2 in Cancer Immunotherapy. Biomed Res Int. 2018;9056173.

59. Schumacher TN, Schreiber RD. Neoantigens in cancer immunotherapy. Science 2015;348:69–74.

60. Pu N, Chen Q, Gao S, Liu G, Zhu Y, Yin L, et al. Genetic landscape of prognostic value in pancreatic ductal adenocarcinoma microenvironment. Ann Transl Med 2019;7:645.

61. Wartenberg M, Cibin S, Zlobec I, et al. Integrated genomic and immunophenotypic classification of pancreatic cancer reveals three distinct subtypes with prognostic/predictive significance. Clin Cancer Res 2018;24:4444–54.

62. Cheng H, Fan K, Luo G, et al. Kras G12D mutation contributes to regulatory T cell conversion through activation of the MEK/ERK pathway in pancreatic cancer. Cancer Lett. 2019;446:103-111.

Figure legends

Fig. 1 Characterization of TLS in PDAC. **a** Representative images of H&E-stained sections were obtained from resected PDAC. The dotted line indicates the margin of the tumor, and the black arrow indicates the TLS beside the tumor (left panel). TLS within the tumor is shown, and black arrowheads indicate cancer cells (right panel). **b & c** Components and proportions of immune cells within TLS. In the IHC analysis, the TLSs were composed of T cells (CD4, CD8, CD45RO, and FOXP3), B cells (CD20), and macrophages (CD68). **d** The association between the presence of TLS and tumor characteristics (pTNM stage, pT stage, and histological grade). Statistical significance was set at $P < 0.05$. Original magnification (a, 40×; b, 200×). Scale bars, 200 μm (a); 50 μm (b). H&E, haematoxylin and eosin; IHC, immunohistochemistry; PDAC, pancreatic ductal adenocarcinoma; TLS, tertiary lymphoid structure

Fig. 2 CSS of the PDAC patients according to the presence or absence of TLS. The CSS of PDAC patients according to the presence or absence of TLS was investigated. The differences of the CSS in adjuvant chemotherapy among the groups treated with S-1, gemcitabine, and non-treated groups according to the

presence or absence of TLS were also examined. **a** All patients **b** TLS-present, and **c** TLS-absent patients. The CSS curves were estimated using the Kaplan-Meier method, and the significant differences between the two groups were evaluated using a log-rank test. The number of patients at risk is shown in the CSS curves. CSS, cancer-specific survival; PDAC, pancreatic ductal adenocarcinoma; TLS, tertiary lymphoid structure

Supplementary Fig. 1 Representative immunohistochemistry images. **a** Typical images of high or low levels of $CD4^+$, $CD8^+$, $CD45RO^+$ and $FOXP3^+$ TILs. **b** Typical images of presence or absence of CD274 (PD-L1) expression. **c** Typical images of intact or altered (lost or over expression) of protein expression of *TP53*, *CDKN2A* and *SMAD4*. Original magnification (a-c, 200×). Scale bars, 50 μm (a-c). PDL1, Programmed death-ligand 1; TILs, tumor infiltrating lymphocytes

Supplementary Fig. 2 CSS of PDAC patients according to the intratumoral TLS and peritumoral TLS. Intratumoral TLSs were detected within and around the tumor; peritumoral TLSs were detected only around the tumor. The CSS curves were estimated using the Kaplan-Meier method, and the significant differences

between the two groups were evaluated using a log-rank test. The number of patients at risk is shown in the CSS curves. CSS, cancer-specific survival; PDAC, pancreatic ductal adenocarcinoma; TLS, tertiary lymphoid structure

Supplementary Fig. 3 CSS of PDAC patients according to the level of NLR or extent of $CD8^+$ TILs. The CSS of PDAC patients according to high or low NLR were investigated. The differences of the CSS in adjuvant chemotherapy among the groups treated with S-1, gemcitabine, and non-treated groups according to the high or low NLR were also examined. **a** All patients **b** Patients with low NLR **c** Patients with high NLR. The CSS of PDAC according to the high or low levels of $CD8^+$ TILs were investigated. The differences of the CSS in adjuvant chemotherapy among the groups treated with S-1, gemcitabine, and non-treated groups according to the high or low levels of $CD8^+$ TILs were also examined. **d** All patients **e** Patients with high levels of $CD8^+$ TILs **f** Patients with low levels of $CD8^+$ TILs. The CSS curves were estimated using the Kaplan-Meier method, and the significant differences between the two groups were evaluated by a log-rank test. The number of patients at risk is shown in the CSS curves. CSS, cancer-specific survival; NLR, neutrophil-to lymphocyte ratio; PDAC, pancreatic

ductal adenocarcinoma; TILs, tumor infiltrating lymphocytes

Supplementary Fig. 4 In situ hybridization for IFN-gamma and IL-2, and apoptosis assay. **a** Typical images of IFN-gamma and IL-2 expression in TLS-present and absent patients. IFN-gamma-positive cells and IL-2-positive cells show distinct red staining. **b** The expression levels of IFN-gamma or IL-2 per cm^2 in TLS-present patients (n=5) and TLS-absent patients (n=5) were counted. Mean ± SD (bars). *, $P < 0.05$. **c** Double immunohistochemistry-in situ hybridization. To distinguish between IHC of $CD4^+$ and $CD8^+$ T cells (brown) and ISH of IFN-gamma (pink) more clearly, brown is changed to green using color replacement tools of Photoshop. IFN-gamma mRNA (pink arrowhead) was localized to $CD4^+$ and $CD8^+$ T cells (green). **d** TUNEL assays were performed 7 days after the addition of IFN-gamma (100 units/mL), IL-2 (500 units/ml), 5-FU (0.05 mg/mL), and their combination to detect the apoptotic cells. TUNEL analysis showed a significant difference in cell numbers at day 7 between the combination therapy group and other treatment groups. Mean ± SD (bars). **, $P < 0.001$, ***, $P < 0.01$. Original magnification (a, c, 400×). Scale bars, 20 μm. IFN, interferon; IL, interleukin; PDAC, pancreatic ductal adenocarcinoma; SD, standard

deviation; TLS, tertiary lymphoid structure

Fig. 1

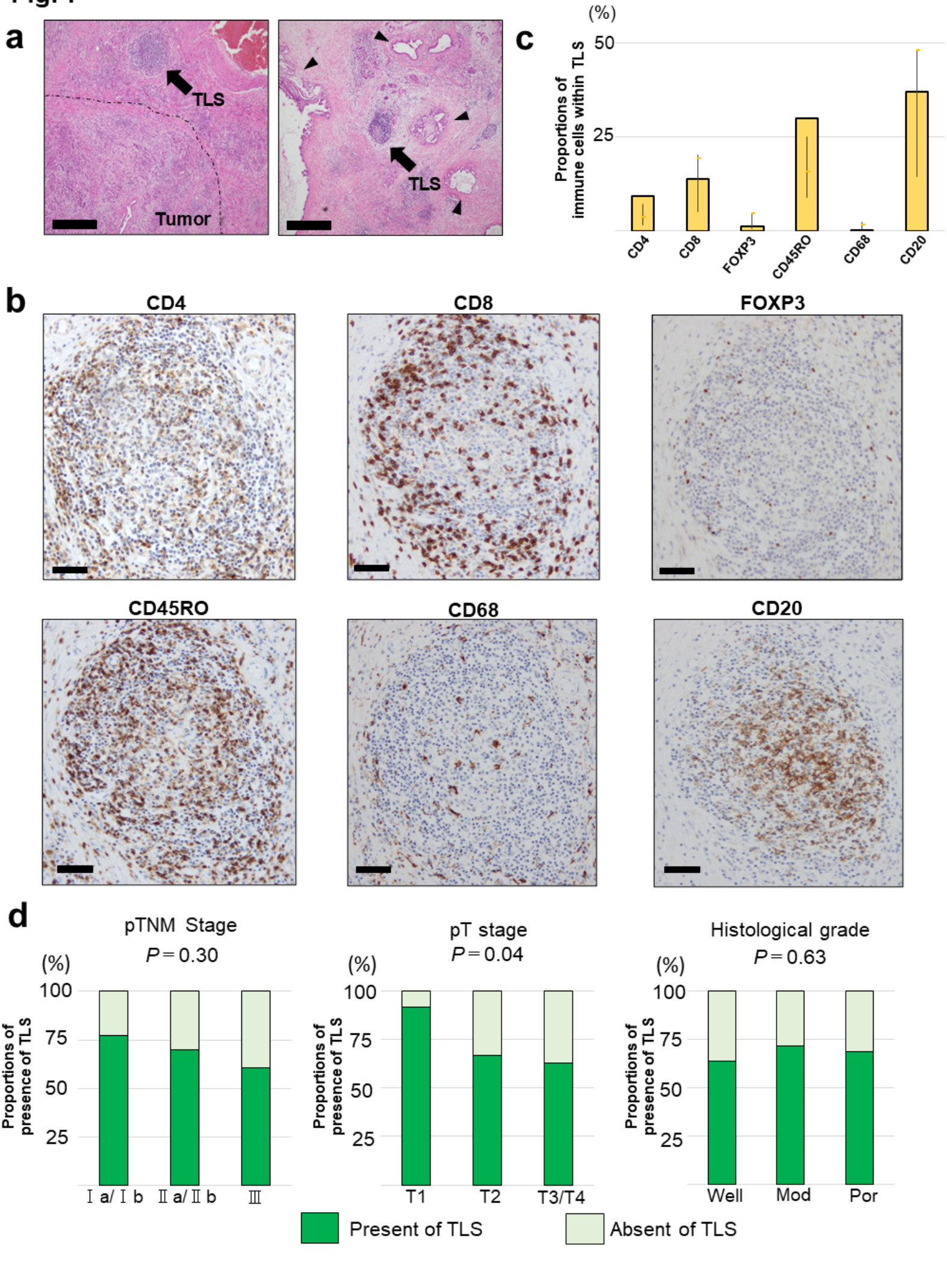
a
TLS
Tumor
TLS
c
(%)
Proportions of immune cells within TLS
50
25
CD4
CD8
FOXP3
CD45RO
CD68
CD20
b
CD4
CD8
FOXP3
CD45RO
CD68
CD20
d
pTNM Stage
P = 0.30
pT stage
P = 0.04
Histological grade
P = 0.63
(%)
100
75
50
25
Proportions of presence of TLS
Ⅰa/Ⅰb
Ⅱa/Ⅱb
Ⅲ
T1
T2
T3/T4
Well
Mod
Por
Present of TLS
Absent of TLS

Fig. 2

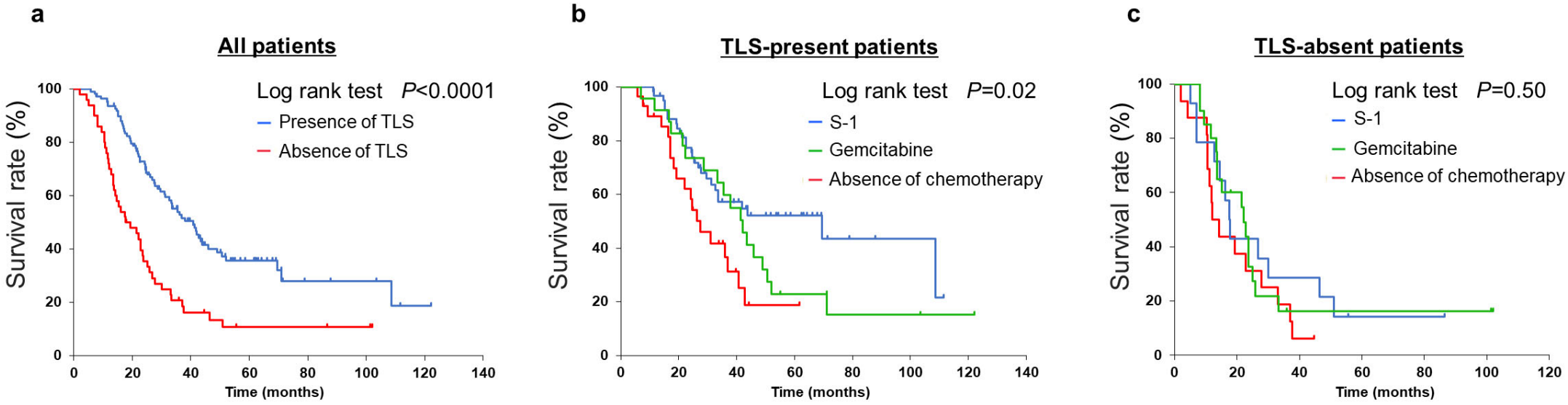

Number of samples

Time (months)	0	20	40	60	80	100	120
TLS presence	112	85	41	18	5	4	1
TLS absence	50	23	7	3	3	2	0

Number of samples

Time (months)	0	20	40	60	80	100	120
S-1	60	49	24	12	3	2	0
Gemcitabin	23	19	12	4	2	1	1
No chemotherapy	29	17	5	2	0	0	0

Number of samples

Time (months)	0	20	40	60	80	100
S-1	14	6	4	1	1	0
Gemcitabin	20	11	2	2	2	2
No chemotherapy	16	6	1	0	0	0

Table 1. Patient's characteristics according to presence or absence of TLS in PDAC

Characteristics	All patients (N=162)	TLS		*P* value
		Present (N=112)	Absent (N=50)	
Age (years), Median (range)	69 (40-85)	70 (40-85)	69 (48-82)	0.66
BMI (kg/m^2), Median (range)	21.0 (14.3-33.2)	21.0 (14.3-32.3)	20.7 (16.5-33.2)	0.92
Sex				0.61
Male	90 (55.6%)	64 (57.1%)	26 (52.0%)	
Female	72 (44.4%)	48 (42.9%)	24 (48.0%)	
Family history of PDAC				0.55
Present	14 (8.6%)	11 (9.8%)	3 (6.0%)	
Absent	148 (91.4%)	101 (90.2%)	47 (94.0%)	
Alcohol consumption				0.15
< 50 (g/day)	146 (90.1%)	98 (87.5%)	48 (96.0%)	
≥ 50 (g/day)	16 (9.9%)	14 (12.5%)	2 (4.0%)	
History of smoking				0.02
Present	78 (48.1%)	61 (54.5%)	17 (34.0%)	
Absent	84 (51.9%)	51 (45.5%)	33 (66.0%)	
Diabetes mellitus				0.99
Present	64 (39.5%)	44 (39.3%)	20 (40.0%)	
Absent	98 (60.5%)	68 (60.7%)	30 (60.0%)	
CA19-9				0.02
< 37 (U/ml)	40 (24.7%)	34 (30.4%)	6 (12.0%)	
≥ 37 (U/ml)	122 (75.3%)	78 (69.6%)	44 (88.0%)	
CEA				0.71
< 5 (ng/ml)	116 (71.6%)	79 (70.5%)	37 (74.0%)	
≥ 5 (ng/ml)	46 (28.4%)	33 (29.5%)	13 (26.0%)	
Pathological Stage[a]				0.30
Ia/Ib	35 (21.6%)	27 (24.1%)	8 (16.0%)	
IIa/IIb	89 (54.9%)	62 (55.4%)	27 (54.0%)	
III	38 (23.5%)	23 (20.5%)	15 (30.0%)	
Neoadjuvant chemotherapy				0.99
Present	18 (11.1%)	13 (11.6%)	5 (10.0%)	
Absent	144 (88.9%)	99 (88.4%)	45 (90.0%)	
Adjuvant chemotherapy				0.45
Present	117 (72.2%)	83 (74.1%)	34 (68.0%)	
Absent	45 (27.8%)	29 (25.9%)	16 (32.0%)	
Histology grade				0.99
Well/Moderate	143 (88.3%)	99 (88.4%)	44 (88.0%)	
Poorly	19 (11.7%)	13 (11.6%)	6 (12.0%)	
Residual tumor status				0.44
R0	118 (72.8%)	84 (75.0%)	34 (68.0%)	
R1	44 (27.2%)	28 (25.0%)	16 (32.0%)	
KRAS mutation				0.99
Present	150 (92.6%)	104 (92.9%)	46 (92.0%)	
Absent	12 (7.4%)	8 (7.1%)	4 (8.0%)	
TP53 alteration				0.86
Present	111 (68.5%)	76 (67.9%)	35 (70.0%)	
Absent	51 (31.5%)	36 (32.1%)	15 (30.0%)	
CDKN2A alteration				0.21
Present	104 (64.2%)	68 (60.7%)	36 (72.0%)	
Absent	58 (35.8%)	44 (39.3%)	14 (28.0%)	
SMAD4 alteration				0.22
Present	62 (38.3%)	39 (34.8%)	23 (46.0%)	
Absent	100 (61.7%)	73 (65.2%)	27 (54.0%)	
CD274 expression				0.002
Positive	23 (14.2%)	9 (8.0%)	14 (28.0%)	
Negative	139 (85.8%)	103 (92.0%)	36 (72.0%)	

(%) indicates the proportion of cases with a specific clinical, pathological, or tumor molecular characteristic according to the presence or absence of TLS.
[a] Pathological stage was diagnosed based on TNM Classification of Malignant Tumors, 8th Edition. BMI, body mass index; CA19-9, carbohydrate antigen 19-9; CEA, carcinoembryonic antigen; PDAC, pancreatic ductal adenocarcinoma; PD-L1, programmed cell death ligand-1; TLS, tertiary lymphoid structure.

Table 2. The association of TLS with TILs in PDAC

		No. of Cases	No. of cases with high levels of $CD4^+$ TILs	**High levels of $CD4^+$ TILs**		
				Univariate OR (95%CI)	Multivariate OR[a] (95%CI)	Multivariate OR[b] (95%CI)
TLS		162	80 (49.4%)			
	Absence	50	14 (28.0%)	1 (reference)	1 (reference)	1 (reference)
	Presence	112	66 (58.9%)	3.69 (1.82-7.80)	4.21 (1.93-9.74)	3.50 (1.65-7.80)
	P value			0.0002	0.0002	0.001
		No. of Cases	No. of cases with high levels of $CD8^+$ TILs	**High levels of $CD8^+$ TILs**		
				Univariate OR (95%CI)	Multivariate OR[a] (95%CI)	Multivariate OR[b] (95%CI)
TLS		162	81 (50.0%)			
	Absence	50	9 (18.0%)	1 (reference)	1 (reference)	1 (reference)
	Presence	112	72 (64.3%)	8.20 (3.76-19.6)	9.15 (3.98-23.1)	11.0 (4.57-29.7)
	P value			<0.0001	<0.0001	<0.0001
		No. of Cases	No. of cases with high levels of $CD45RO^+$ TILs	**High levels of $CD45RO^+$ TILs**		
				Univariate OR (95%CI)	Multivariate OR[a] (95%CI)	Multivariate OR[b] (95%CI)
TLS		162	81 (50.0%)			
	Absence	50	17 (34.0%)	1 (reference)	1 (reference)	1 (reference)
	Presence	112	64 (57.1%)	2.59 (1.31-5.27)	2.51 (1.19-5.46)	2.65 (1.25-5.80)
	P value			0.006	0.02	0.01
		No. of Cases	No. of cases with high levels of $FOXP3^+$ TILs	**High levels of $FOXP3^+$ TILs**		
				Univariate OR (95%CI)	Multivariate OR[a] (95%CI)	Multivariate OR[b] (95%CI)
TLS		162	76 (46.9%)			
	Absence	50	23 (46.0%)	1 (reference)	1 (reference)	1 (reference)
	Presence	112	53 (47.3%)	1.05 (0.54-2.07)	0.86 (0.40-1.81)	0.80 (0.45-1.83)
	P value			0.88	0.68	0.80

Lymphocyte counts were divided into high and low group by the median split. The median of $CD4^+$, $CD8^+$, $CD45RO^+$ and $FOXP3^+$ T cells are 48, 140, 110 and 33 count/mm^2, respectively.
[a] The odds ratio was initially adjusted for age, sex, BMI, amount of alcohol consumption, family history of pancreatic cancer, history of smoking, diabetes mellitus, serum CA19-9, serum CEA.
[b] The odds ratio was initially adjusted for stage, histology, adjuvant, neo-adjuvant, residual tumor status, gene alterations (*KRAS*, *TP53*, *CDKN2A*, *SMAD4*).
OR, odds ratio; PDAC, pancreatic ductal adenocarcinoma; TILs, tumor-infiltrating lymphocytes; TLS, tertiary lymphoid structure.

Table 3. The association of TLS with serum ALC, ANC and NLR in PDAC

				High levels of serum ALC		
		No. of cases	No. of cases with high levels of ALC	Univariate OR (95%CI)	Multivariate OR[a] (95%CI)	Multivariate OR[b] (95%CI)
TLS		162	81 (50.0%)			
	Absence	50	17 (34.0%)	1 (reference)	1 (reference)	1 (reference)
	Presence	112	64 (57.1%)	2.59 (1.31-5.27)	2.84 (1.33-6.28)	2.46 (1.21-5.12)
	P value			0.006	0.007	0.01
				High levels of serum ANC		
		No. of cases	No. of cases with high levels of ANC	Univariate OR (95%CI)	Multivariate OR[a] (95%CI)	Multivariate OR[b] (95%CI)
TLS		162	80 (49.4%)			
	Absence	50	24 (48.0%)	1 (reference)	1 (reference)	1 (reference)
	Presence	112	56 (50.0%)	1.08 (0.56-2.12)	1.33 (0.64-2.75)	1.11 (0.54-2.30)
	P value			0.81	0.44	0.78
				Low levels of NLR		
		No. of cases	No. of cases with low levels of NLR	Univariate OR (95%CI)	Multivariate OR[a] (95%CI)	Multivariate OR[b] (95%CI)
TLS		162	80 (49.4 %)			
	Absence	50	15 (30.0%)	1 (reference)	1 (reference)	1 (reference)
	Presence	112	65 (58.0%)	3.23 (1.61-6.72)	3.21 (1.51-7.10)	3.15 (1.53-6.72)
	P value			0.0009	0.002	0.002

ALC and ANC counts and NLR were divided into high and low categories by the median split. The median of ALC and ANC were 1522 and 3251 count/mm^2, respectively. The median of NLR was 2.1.

[a] The odds ratio was initially adjusted for age, sex, BMI, amount of alcohol consumption, family history of pancreatic cancer, history of smoking, diabetes mellitus, serum CA19-9, serum CEA.

[b] The odds ratio was initially adjusted for stage, histology, adjuvant, neo-adjuvant, residual tumor status, gene alterations (*KRAS, TP53, CDKN2A, SMAD4*).

ALC, absolute lymphocyte counts; ANC, absolute neutrophil counts; NLR, neutrophil-to lymphocyte ratio; OR, odds ratio; PDAC, pancreatic ductal adenocarcinoma; TLS, tertiary lymphoid structure.

Table 4. Presence of TLS and cancer specific mortality in PDAC

	No. of cases	No. of events	Pancreatic cancer specific mortality		
			Univariate HR (95%CI)	Multivariate HR[a] (95%CI)	Multivariate HR[b] (95%CI)
All cases	162	107			
TLS absence	50	43	1 (reference)	1 (reference)	1 (reference)
TLS presence	112	64	0.40 (0.27-0.59)	0.40 (0.26-0.61)	0.37 (0.25-0.56)
P value			<0.0001	<0.0001	<0.0001
Pathological stage IIb-III[c]	119	88			
TLS absence	40	37	1 (reference)	1 (reference)	1 (reference)
TLS presence	79	51	0.34 (0.22-0.53)	0.35 (0.22-0.56)	0.33 (0.21-0.52)
P value			<0.0001	<0.0001	<0.0001

[a] The hazard ratio was initially adjusted for age, sex, BMI, amount of alcohol consumption, family history of pancreatic cancer, history of smoking, diabetes mellitus, serum CA19-9, serum CEA.
[b] The hazard ratio was initially adjusted for stage, histology, adjuvant, neo-adjuvant, residual tumor status, gene alterations (*KRAS*, *TP53*, *CDKN2A*, *SMAD4*).
[c] Pathological stage was diagnosed based on TNM Classification of Malignant Tumors, 8th Edition.
HR, hazard ratio; PDAC, pancreatic ductal adenocarcinoma; TLS, tertiary lymphoid structure.

Table 5. Adjuvant chemotherapy and patient mortality in PDAC

				Pancreatic cancer specific mortality			
	Adjuvant chemotherapy	No. of cases	No. of events	Univariate HR (95%CI)	*P* value	Multivariate HR (95%CI)	*P* value
TLS Presence	Absent	29	19	1 (reference)		1 (reference)	
	S-1	60	27	0.43 (0.24-0.79)	0.007	0.51 (0.26-0.97)	0.04
	GEM	23	18	0.66 (0.34-1.28)	0.21	0.60 (0.29-1.26)	0.18
TLS Absence	Absent	16	15	1 (reference)		1 (reference)	
	S-1	14	12	0.66 (0.30-1.42)	0.28	0.61 (0.27-1.37)	0.23
	GEM	20	16	0.71 (0.35-1.46)	0.35	0.67 (0.27-1.37)	0.30

The hazard ratio was initially adjusted for age, BMI, history of smoking, residual tumor status. BMI, body mass index; GEM, gemcitabine; HR, hazard ratio; PDAC, pancreatic ductal adenocarcinoma; TLS, tertiary lymphoid structure.